

Matematisk-fysiske Meddelelser
udgivet af
Det Kongelige Danske Videnskabernes Selskab
Bind **33**, nr. 13

Mat. Fys. Medd. Dan. Vid. Selsk. **33**, no. 13 (1963)

THE REACTION $\text{Ne}^{20}(\alpha, \text{C}^{12})\text{C}^{12}$

BY

N. O. LASSEN AND JANUS STAUN OLSEN



København 1963
i kommission hos Ejnar Munksgaard

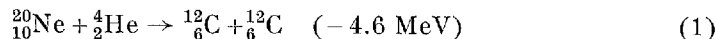
Synopsis

Natural neon was bombarded by α -particles with laboratory energies ranging from 12 to 20 MeV. The neon gas serving as target was used at the same time as filling gas for a gridded, electron collection type ionization chamber used to measure the emitted carbon ions.

The differential cross section at C.M. angle 90° was measured as a function of energy; the excitation curve shows several peaks (Fig. 10). The angular distributions were measured for each of these peaks (Fig. 12). One distribution follows a $[P_8(\cos \theta)]^2$ curve; this peak may correspond to a single $8+$ state in the compound Mg^{24} nucleus at 25.2 MeV excitation energy, having $I < 150$ keV. The other angular distributions also show strong maxima and minima, but at least two even angular momentum states must contribute to each peak. It is believed that a somewhat larger number of states participate in the reaction, statistical variations in this number being responsible for the appearance of the excitation curve.

1. Introduction

At the International Conference on Nuclear Structure, Kingston, Canada, in the autumn of 1960, results obtained by ALMQVIST, BROMLEY and KÜEHNER¹⁾ of the elastic scattering of carbon ions and of the reaction $^{12}_6\text{C} (^{12}_6\text{C}, \alpha) ^{20}_{10}\text{Ne}$ were reported. These authors found peculiar resonances in the elastic C-C process for ion energies above the Coulomb barrier and in some reaction processes for energies just below the barrier. Therefore, it might be expected that also the reaction



would show interesting features, and it was decided to make a study of this process by means of the α -beam from the Copenhagen cyclotron.

Since the energy of our α -particles is 20 MeV, carbon ions with an energy of about 6 MeV in the C.M. system are produced in reaction (1). An apparatus was constructed by means of which these fission carbon ions could be detected²⁾. The principle of the method was to use an ionization chamber filled with neon to such a pressure that the short range heavily ionizing fission ions were stopped inside the chamber, giving pulses corresponding to their full energy, whereas α -particles and other lighter ions coming from the target spent only a small part of their range in the chamber and thus gave only small pulses. At the same time the neon gas acted as the target, the α -beam being passed across the ionization chamber inside a tube with small side holes.

In three separate experiments with different tubes the number of fission ions at the lab. angles 90° , 62° and 58° were counted. Search for other modes of fission than reaction (1) was made, but none were seen. A search for the reaction $^{28}_{14}\text{Si} (\alpha, 0^{16}) 0^{16}$ was also made, using SiH_4 in the chamber³⁾, but neither was this process seen.

The results for reaction (1) indicated a strong angular variation of the cross section. To measure the angular distribution in more detail an apparatus based on the same principle, but having a different geometry, was

built; it will be described in the present paper. Preliminary results have been briefly reported⁴⁾.

It was soon found that the cross section was also varying strongly with the energy of the α -particles. Therefore it was necessary to construct a device for measuring the α -energy continuously during the experiments in order to ensure that it remained constant. With this energy monitor in use,

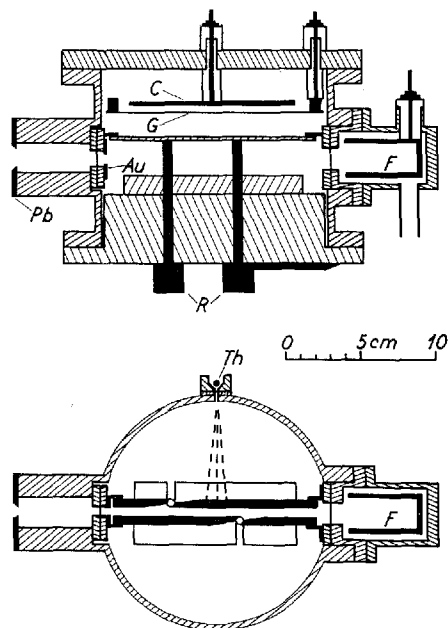


Fig. 1. The neon chamber. The α -beam is limited by the lead stop Pb and the (defining) gold stop Au, and it is measured by the evacuated Faraday cup F. G is a Frisch grid, C collector electrodes, and Th a source of natural α -particles used for calibration. R are two rotatable brass rods carrying the channels which define the emission angles of the carbon ions. Vertical (upper) and horizontal (lower) sections are shown.

an excitation curve was obtained with a somewhat different geometry for C^{12} detection, in which particles emitted in a wide angular range, approximately 20° – 160° , were registered. The excitation curve showed marked resonances⁵⁾. However, the wide angular range involved a rather thick target; furthermore, by the geometry the different angles had different detection efficiencies. Therefore, it was realized that a better way to find an excitation function might be to measure the differential cross section for $\theta = 90^\circ$ as a function of energy.

The present paper deals with such measurements as well as with measurements of the angular distribution for a number of resonances.

2. Experimental apparatus

The carbon ions were detected by means of a gridded ionization chamber. Part of the apparatus is shown in Fig. 1. The ionization chamber is housed in a steel tube with 150 mm inside diameter. The α -beam traverses the tube along a diameter; it enters through a side tube carrying a lead plate with a hole, $6 \times 11 \text{ mm}^2$. A nickel foil, 1 mg/cm^2 thick, separates the chamber

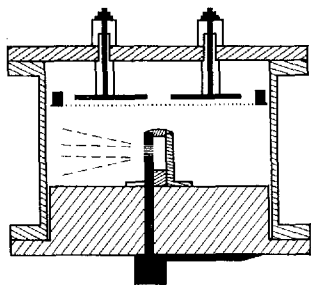


Fig. 2. Section through the neon chamber perpendicular to the beam.

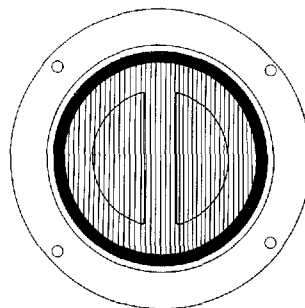


Fig. 3. View of the electrode system.

from the cyclotron vacuum; the window is $6 \times 11 \text{ mm}^2$, but just behind it is placed a gold diaphragm which reduces the beam cross section to $5 \times 10 \text{ mm}^2$. Right opposite the entrance tube another side tube housing a Faraday cup is placed; it is connected to the cyclotron vacuum through a rubber tube, and is separated from the ionization chamber by means of a tantalum foil of thickness $\sim 20 \text{ mg/cm}^2$; this window is circular and 15 mm in diameter. Inside the chamber the α -beam passes through a duct so that, from the active volume of the ionization chamber outside this duct, the beam can be seen only through some narrow channels in the side walls.

Fig. 2 shows a vertical cross section perpendicular to the beam direction, and Fig. 3 shows the electrodes of the ionization chamber viewed from below. The grid consists of parallel 0.15 mm platinum wires, spaced 3 mm, and held by a brass ring supported by three teflon insulators (one of them shown in Fig. 1). There are two collector electrodes, each connected to its own preamplifier; thus, there are actually two ionization chambers.

The duct is made of four pieces of dural screwed to the bottom plate and placed very accurately; on top is a lid. At the two ends special shields

are placed, and the only openings left are the actual emission channels in two circular brass rods placed in the side walls of the duct in the way shown in Fig. 1 and, in more detail, in Fig. 4. The rods can be rotated from outside and their position can be read by means of a pointer and a scale; the vacuum seal is provided by o-rings. The rods are 5.0 mm in diameter; the upper end of each rod is made of two half circular pieces screwed to-

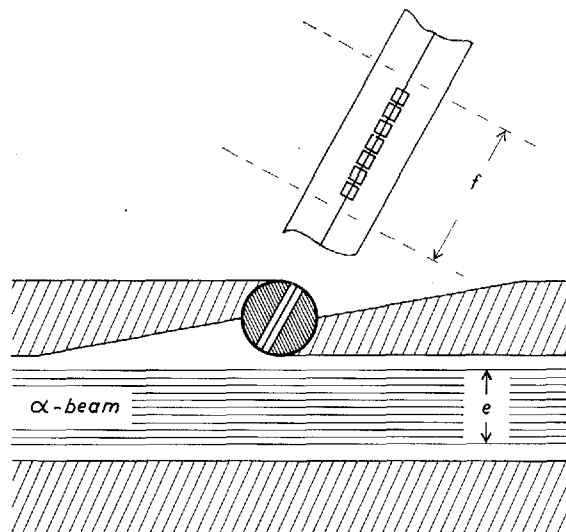


Fig. 4. Details of a rod with channels. e and f denote the horizontal and vertical extensions of the α -beam. $e = 0.5$ cm. $f = 1.0$ cm. A cross section and a side view of a rod are shown.

gether, and between them is a 0.1 mm bronze foil separating the two rows of channels cut in the pieces. There are 14 channels in each rod, each channel 0.5×1.0 mm² in cross section. To obtain a higher angular resolution some measurements of the angular distribution were made by using rods with narrower channels; each of these rods had 28 channels (in four rows) of cross section 0.2×1.0 mm².

The chamber was filled with pure neon. In our earlier experiments, a few percent of methane had been added, but to avoid trouble from recoil carbon ions, pure neon was used in the present experiment. The chamber was found to work equally well without CH₄ and with much lower voltages. Mostly, neon pressures of the order of 200 mm of Hg were used, and the voltage on the collector electrode was 100 V; at very low neon pressures

(<50 mm) the voltage had to be lower. The gas was continuously purified by circulation over hot calcium in a side tube.

Via a standard amplifier the chamber was connected to a 100-channel pulse height analyzer. Calibration was made by $\text{ThC} + \text{C}'$ α -particles crossing the chamber in a well collimated beam. The particles were stopped by hitting the duct; they dissipated an energy of the order of 1 MeV in the chamber. The energy resolution (full width at half maximum height) was about 8%, approximately what should be expected from straggling. For

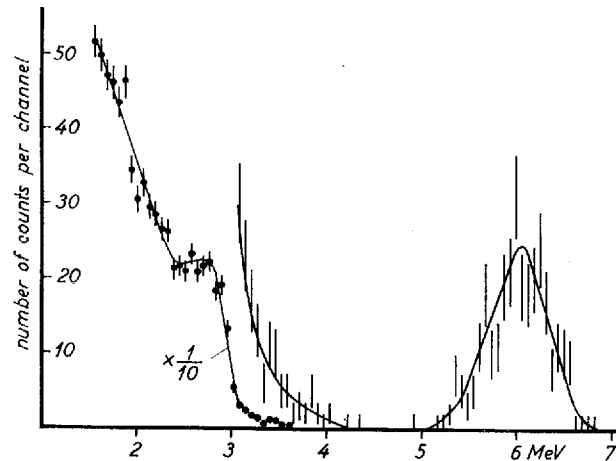


Fig. 5. Pulse height distribution showing a peak at 6 MeV corresponding to C^{12} ions. The spectrum was obtained with 0.5μ Coulomb of 19.5 MeV α -particles and $\vartheta_{\text{Lab}} = 62^\circ$. The neon pressure was 300 mm of Hg.

emission angles in the range $20^\circ < \vartheta < 80^\circ$ the fission ions gave a peak in the energy distribution curve well separated from the background; an example is seen in Fig. 5.

The energy of the α -particles was changed by means of absorbers, and it was measured by another gridded ionization chamber connected to another 100-channel pulse height analyzer. The analyzed⁶⁾ beam from the cyclotron was passed through a lead diaphragm with a hole, 22 mm in diameter (Fig. 6). Behind it three foil holders were placed in a slide arrangement; each could be set in four different positions and, in this way, different absorber thicknesses could be introduced in the beam. The absorber foils were 25 mm in diameter. Some were of nickel, the thicknesses being multiples of 0.5 mg/cm^2 ; others were of beryllium, in multiples of 5 mg/cm^2 .

Also Al foils were used. To cover the energy range 12–20 MeV several sets of foil holders were used. Behind the foils a second, vertically adjustable, lead diaphragm reduced the beam cross section to $5 \times 10 \text{ mm}^2$, and behind it the beam passed through a 0.16 mg/cm^2 gold foil, placed at an angle of 45° . The elastically scattered α -particles from this foil were registered by the α -ionization chamber; it was similar in construction to a chamber earlier described⁸⁾. It was filled with argon to about three atmospheres with

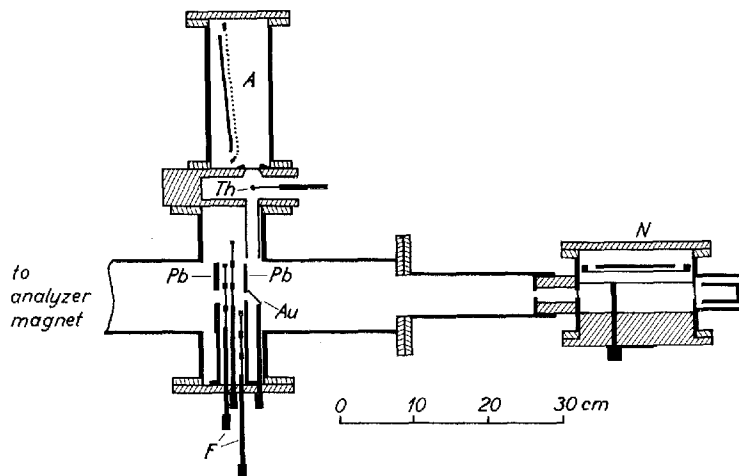


Fig. 6. The experimental arrangement.

N: Neon chamber. A: Ionization chamber for measurement of energy of scattered α -particles. Pb: Lead stops. F: Movable holders with absorber foils. Au: Gold scattering foil. Th: Removable source of natural α -particles.

an admixture of a few percent methane; the gas was continuously purified by circulation over hot calcium. The resolution for ThC α -particles was 2%, or 160 keV. For some unknown reason, maybe because the width of the chamber was insufficient, the resolution was slightly inferior for the scattered α -particles, about 250–300 keV. Other measurements by solid-state counters have indicated that the energy spread of the undegraded beam was about 70 keV.

The thinnest Ni foil reduced the α -energy by 70–100 keV. Smaller changes were sometimes obtained by deliberately changing the Dee positions or other cyclotron parameters. The energy of the α -particles at the target could also be varied by changing the pressure in the neon chamber and thus the absorption in the neon gas in front of the target volume.

3. Evaluation of the differential cross sections from the measured numbers

Figs. 7 and 8 show the geometry. We first want to find the number of carbon ions escaping through one channel. Suppose the channels are set at an angle ϑ_0 . We take the horizontal plane through the channel as xy-plane (Fig. 7). Consider such particles in this plane which move in directions having angles in the interval $\vartheta_0 + \Delta\vartheta < \vartheta < \vartheta_0 + \Delta\vartheta + d\vartheta$ (here, for the

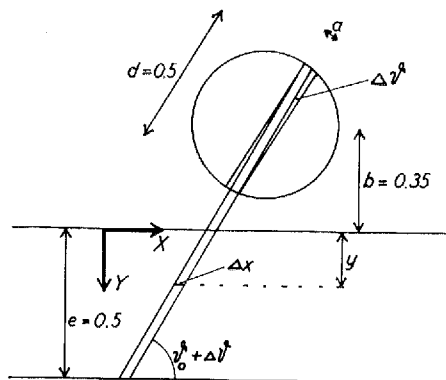


Fig. 7. Horizontal section through a channel.

present considerations $\Delta\vartheta$ is a fixed angle). If they are to escape through the channel, they must start within a region of the target having the thickness

$$\Delta x = \frac{a - |\Delta\vartheta \cdot d|}{\sin(\vartheta_0 + \Delta\vartheta)}, \quad (2)$$

where a and d are the width and the length of the channel.

If they start from the depth y they have to be emitted within a solid angle

$$d\omega = \frac{rd\vartheta \cdot h}{r^2} \quad (3)$$

where h is the height of the channel and where

$$r = \frac{d}{2} + \frac{b + y}{\sin(\vartheta_0 + \Delta\vartheta)}, \quad (4)$$

b having the meaning shown in Fig. 7.

However, it is necessary to take into account also the z -dimension. Consider a line element of target parallel to the x -axis and having coordinates y and z . If $|z|$ is not too high, particles may escape with a scattering angle $\vartheta_o + \Delta\vartheta$; to a first approximation the target thickness corresponding to such particles is again given by (2), the scattering angle and its projection on the xy -plane not differing much from each other.

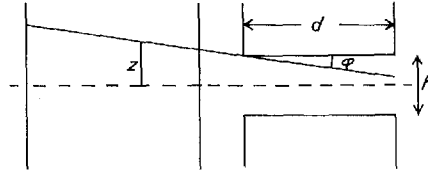


Fig. 8. Vertical section through a channel.

For $|z| > \frac{1}{2}h$, the solid angle is (Fig. 8)

$$d\omega = \frac{rd\vartheta(h - |\varphi d|)}{r^2}, \quad (5)$$

where

$$r = \left[\frac{d}{2} + \frac{b+y}{\sin(\vartheta_o + \Delta\vartheta)} \right] \cdot \frac{1}{\cos \varphi} \approx \frac{d}{2} + \frac{b+y}{\sin(\vartheta_o + \Delta\vartheta)} \quad (6)$$

$$\varphi \approx \operatorname{tg} \varphi = \frac{|z| - \frac{1}{2}h}{\frac{b+y}{\sin(\vartheta_o + \Delta\vartheta)} - \frac{d}{2}} < \frac{h}{d} = \frac{1}{5}. \quad (7)$$

For $|z| < \frac{1}{2}h$ the solid angle is given by (3).

For the angle $\vartheta_o + \Delta\vartheta$ the yield from the line element is

$$d^3Y = \left(\frac{d\sigma}{d\omega} \right)_{\vartheta = \vartheta_o + \Delta\vartheta} \cdot 2 \cdot \frac{n dy dz}{ef} \cdot N \Delta x \cdot d\omega, \quad (8)$$

where N is the number of Ne^{20} atoms per cm^3 of target gas, n is the number of α -particles having passed the total beam cross section of breadth e ($= 0.5$ cm) and height f ($= 1$ cm); Δx is given by (2), $d\omega$ by (3) or (5), and the factor 2 enters because two identical particles are created in the fission process.

Inserting $a = 0.05$, $h = 0.1$ and $d = 0.5$, one finds

$$d^2 Y = 2 \int_{z=0}^{z=\frac{1}{2}h} d^3 Y + 2 \int_{z=\frac{1}{2}h}^{z=z_{\max}} d^3 Y = 0.001 \cdot k_1 \cdot \frac{1 - 10 \cdot |\Delta\vartheta|}{\sin(\vartheta_0 + \Delta\vartheta)} d\vartheta dy, \quad (9)$$

where $z_{\max} = \varphi_{\max} \frac{b+y}{\sin(\vartheta_0 + \Delta\vartheta)} = \frac{1}{5} \frac{b+y}{\sin(\vartheta_0 + \Delta\vartheta)}$, and $k_1 = \frac{2nN}{ef} \frac{d\sigma}{d\omega}$, the cross section $\frac{d\sigma}{d\omega}$ being assumed to be constant for all possible values of $\Delta\vartheta$ corresponding to a fixed ϑ_0 . By further integrating between the limits $y = 0$ and $y = 0.5$, one gets

$$dY = 0.0005 k_1 \frac{1 - 10 \cdot |\Delta\vartheta|}{\sin(\vartheta_0 + \Delta\vartheta)} d\vartheta. \quad (10)$$

Fig. 9 shows, for $\vartheta_0 = 30^\circ$, this value dY as a function of $\vartheta = \vartheta_0 + \Delta\vartheta$. The distribution is almost a triangle. If we are interested merely in the total area, we may just as well replace the denominator $\sin(\vartheta_0 + \Delta\vartheta)$ by simply the constant value $\sin \vartheta_0$. Integration of (10) then gives

$$Y(\vartheta_0) = 2 \int_0^{\Delta\vartheta_{\max}} dY = 0.00005 \cdot \frac{k_1}{\sin \vartheta_0} = \frac{1}{\sin \vartheta_0} \cdot 0.0002 nN \cdot \frac{d\sigma}{d\omega}.$$

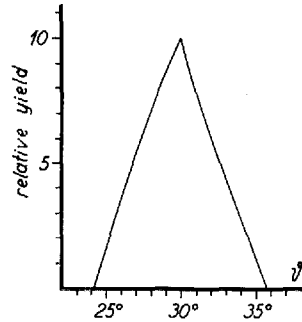


Fig. 9. Approximate response curve for channels set at $\vartheta_0 = 30^\circ$. A correction to the curve is given in the text.

Taking into account the number of channels one finds for the number of carbon ions

$$n_c = 28 \cdot 10^{-4} \cdot \frac{1}{\sin \vartheta_0} \cdot nN \frac{d\sigma}{d\omega}.$$

From this expression the differential cross section in the lab. system is found. The C.M. cross section is found in a well-known way⁷⁾.

The distribution given by (10) and shown in Fig. 9 is not correct. If we want to consider the actual distribution we cannot use the approximation in which the angle and its projection on the xy -plane are put equal. If ϑ is the angle in the xy -plane, φ the inclination and ϑ' the actual angle, then $\cos \vartheta' = \cos \vartheta \cos \varphi$. For $\vartheta = 30^\circ$ and $|\varphi| = \varphi_{\max} = \frac{1}{5}$ this gives $\vartheta' = 32^\circ$. In this example, the center of gravity of the distribution is displaced 0.7 , so instead of being 29.8 as in Fig. 9, it is about 30.5 . Thus for small angles, and especially when the higher angular resolution is used, a correction to the angle is needed (note: $\vartheta = 30^\circ$ corresponds to $\Theta_{\text{cm}} \sim 45^\circ$).

4. Results and discussion

By setting the channels at the proper angle, slightly dependent on α -energy, and counting the number of carbon ions with various foils interposed in the beam, the excitation curve giving $\frac{d\sigma}{d\omega}$ for $\Theta_{\text{cm}} = 90^\circ$ was obtained (Fig. 10). Like the earlier curve⁵⁾ it shows a number of peaks, the positions of which are, as a rule but not always, the same in the two curves; the peaks at 12.6, 13.6, 16.0 and 16.3 from the earlier curve occur in Fig. 10 at 12.7, 13.4, 15.9 and 16.2. However, the two curves are not identical and they should not be so, because they deal with different quantities. The earlier curve was obtained by counting ions in a wide angular range, and it thus gives the variation of the "total" cross section, whereas the present curve refers to the differential cross section at a certain angle. Since the angular distribution is not isotropic, and since it is not the same for different energies, the two quantities must vary with energy in different ways. In fact, it is surprising that the two curves are so much alike, and it may indicate that, although the angular distribution varies with energy, this variation may be rather smooth.

One demonstration of the difference is the fact that we were unable to find for $\Theta = 90^\circ$ any peak corresponding to the pronounced maximum in the "total" yield curve at 14.3 MeV. The observation that the excitation function for $\Theta \sim 45^\circ$ has a sharp peak at this energy is noteworthy, and it is in accordance with the angular distribution (Fig. 12).

Another demonstration may be the smaller widths of the peaks in Fig. 10 compared to the earlier curve; however, the earlier geometry involved a

somewhat larger effective target thickness, which is responsible for part of the increase in width. The difference between the two curves with respect to relative heights of the various peaks is more significant.

As regards the reliability of the curve in Fig. 10, we think that it is substantially correct for energies above 12 MeV. For lower energies the measurements become difficult, because the thick degrader foils and the ensuing rather large compound scattering results in a considerable reduction of the

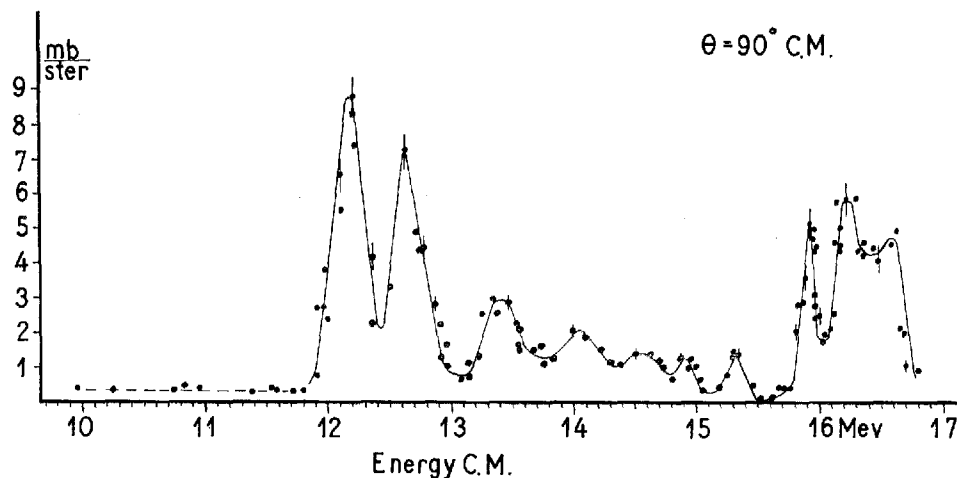


Fig. 10. Differential cross section for the $\text{Ne}^{20}(\alpha, \text{C}^{12})\text{C}^{12}$ reaction at C.M. angle 90° .

part of the beam which enters the neon chamber through the various stops. Since furthermore the fission cross section is rather small below 12 MeV, only few pulses were recorded. Additional troubles arise because, at these low energies of the incoming α -particles, the pulse height spectrum from the neon ionization chamber does not show a carbon peak which is well separated from the background of other pulses. This background has a tail extending to energies higher than the carbon energies, probably caused partly by processes in the chamber initiated by neutrons from the beryllium absorber foils. For these reasons, some ambiguity is involved in the estimation of the fission cross section below 12 MeV. For the inverse process the Chalk River group⁸⁾ has, for energies corresponding in our scale to 10–11 MeV, found an almost constant cross section of about 0.1 mb/ster. The present estimations give 0.3 mb/ster.

A peculiar feature of the curve is the non-existence of resonances below 12 MeV and the rise in the fission cross section at this energy. Part of the

explanation may be that at lower energies the low penetrability through the Coulomb barrier between the two carbon nuclei prevents fission from competing successfully with other modes of decay of the compound nucleus. In this connection, a comparison with the C-C elastic scattering curve measured at Chalk River^{1) 8)} is interesting (see Fig. 11). The prominent peak that we find at 12.1 MeV is just barely seen in the elastic scattering, but, apart from this, there is a very close agreement between the resonance values found in the two experiments.

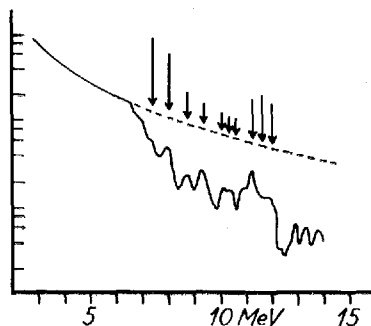


Fig. 11 The curve shows the cross section for elastic $C^{12}-C^{12}$ scattering at C.M. angle 90° as a function of C.M. carbon energy, as obtained by the Chalk River group¹⁾. Arrows indicate positions and amplitudes of our peaks for the $Ne^{20}(\alpha, C^{12})C^{12}$ reaction.

In Fig. 10 the narrowest peak is the one at 15.9 MeV; it has a half width of 145 keV or, when the α -energy is measured in the lab. system, 175 keV. This is presumably somewhat more than the energy spread of the beam having passed the degrader foils, the window and the neon gas in front of the target volume. Also the two peaks between 12 and 13 MeV show half widths (~ 300 keV C.M.) somewhat larger than the estimated straggling in the beam. Comparing the cross sections from Fig. 10 with the elastic C-C cross sections, one can obtain rough estimates for the ratio Γ_c/Γ_α of the partial widths for emission of carbon nuclei and of α -particles; for the 15.9 MeV resonance one finds $\Gamma_c \sim 6 \Gamma_\alpha$.

Fig. 12 shows the angular distributions for the various peaks in Fig. 10 and for one energy (14.3 MeV) at which the "total" cross section (the earlier curve) has a peak, but Fig. 10 has none. When obtaining these distributions, the energy of the incoming α -particles was measured simultaneously with the measurement of each point, and the mean energy was constant to better than ± 30 keV. When the angle is changed by rotating the rod, the position

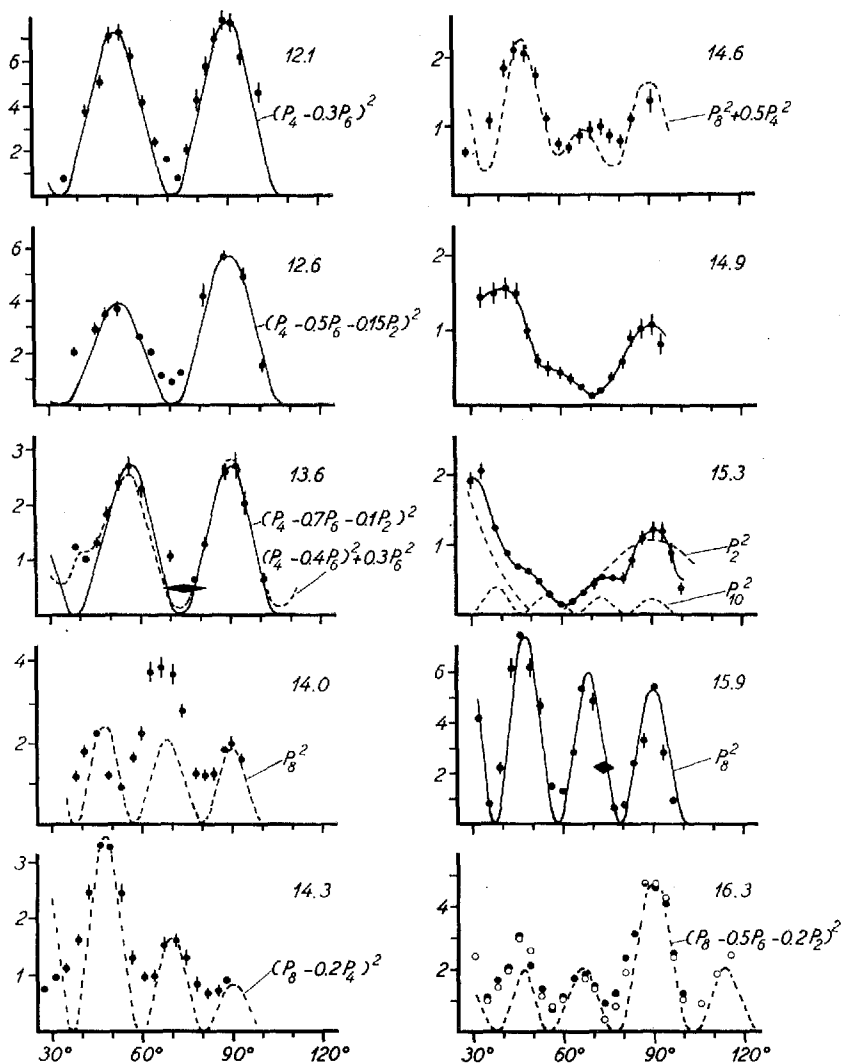


Fig. 12. Angular distributions of carbon ions from the reaction $\text{Ne}^{20}(\alpha, \text{C}^{12})\text{C}^{12}$ at various C.M. energies (entrance channel) written in the figure. For one point in the 13.6 MeV distribution the approximate angular response function for the channels is indicated. One distribution, for 15.9 MeV, was measured with a higher angular resolution, again indicated for one point.

of the target volume is shifted, and therefore the mean energy of the reacting α -particles is slightly altered. However, this effect was compensated by varying the pressure in the neon chamber.

Since the reaction particles, in both the entrance and exit channels, are spinless and all have positive parity, and since two identical particles are emitted, the compound states which may be involved must have even parity and even angular momentum. If the reaction goes through a single level in the compound nucleus, the angular distribution will follow a $[P_l(\cos \theta)]^2$ curve. This is considered to be true for the α -energy 15.9 MeV, and it is inferred that this peak corresponds to a $8+$ level in the compound Mg^{24} nucleus at excitation energy 25.2 MeV and with a total width smaller than 150 keV.

The situation is not so clear for any of the other peaks, and it may be concluded that each peak covers more than one level. If two levels contribute to a peak, the angular distribution will be described by a combination of two even Legendre polynomials. If the levels do not overlap, but lie so close together that the spread in the α -energy prevents their resolution, the angular distribution will be given by

$$\frac{d\sigma}{d\Omega} \sim (P_{l_1})^2 + a_2(P_{l_2})^2, \quad (11)$$

a_2 being real and positive, l_1 and l_2 even. If the levels overlap, the distribution will be

$$\frac{d\sigma}{d\Omega} \sim (\alpha_1 P_{l_1} + \alpha_2 P_{l_2})^2. \quad (12)$$

If in formula (12) the coefficients are real, the distribution will have zero points. In other cases there are generally no zero points. Of course, the limited angular resolution tends to fill out the valleys; however, in some cases the experimental points approach the axis of abscissae, whereas for other α -energies the valleys are not so deep.

The angular distributions in Fig. 12 may be divided into four groups. The three first distributions for 12.1, 12.6 and 13.6 MeV have two maxima between 30° and 100° . The second group, for energies 14.0, 14.3 and 14.6 MeV, have three maxima and not very deep valleys. The third group, 14.9 and 15.3 MeV, have three or four maxima, one deep minimum, the other minima not being so deep. The fourth group, 15.9 and 16.3 MeV, resembles the second by having three maxima, but deviates by having two deep minima in between.

For 12.1 MeV the cross section is very low for 35° and 75° . We conclude that the distribution is of type (12) with real coefficients, corresponding to (at least) two levels so broad that they overlap. In fact,

the curve $(P_4 - 0.3 P_6)^2$ fits nicely the experimental points, indicating levels with $l = 4$ and $l = 6$.

The 12.6 and 13.6 MeV peaks have angular distributions resembling that of the 12.1 MeV peak. This points to levels with the same angular momenta, $l = 4$ and $l = 6$. For the 13.6 MeV peak the curve corresponding to (12) with $\alpha_4 = 1$ and $\alpha_6 = -0.4 + 0.55 i$ fits the experimental points, if the 70° point is disregarded. However, the distribution may be equally well fitted with $(P_4 - 0.7 P_6 - 0.1 P_2)^2$. Therefore, it is not possible to conclude that only two levels contribute, there might also be a level with $l = 2$. For similar reasons, although the curve $(P_4 - 0.5 P_6 - 0.15 P_2)^2$ fits the 12.6 distribution, it cannot be concluded that three levels contribute to the peak.

The second group of angular distributions, for the energies 14.0, 14.3 and 14.6 MeV, cannot be fitted with combinations of P_4 and P_6 , but a P_8 must be involved. Since the distributions have no zero points, attempts were made to fit them with curves of type (11), but with little success. For the 14.6 MeV distribution a curve $P_8^2 + 0.5 P_4^2$ reproduces roughly the three maxima between 30° and 100° , but it is not considered to give a satisfactory fit to the points.

Attempts to fit the 14.9 and 15.3 MeV distributions by curves of type (11) or type (12) by using real coefficients were also unsuccessful. The 15.3 MeV distribution seems to indicate a contribution from angular momentum of at least 10, but due to the small cross section the uncertainties are rather large, and a too detailed analysis would not seem justified.

The last group for energies 15.9 and 16.3 MeV has distributions dominated by $l = 8$. It may be mentioned that, although the 15.9 MeV peak shows a pure P_8^2 distribution, it may nevertheless contain more than one level, if only all significantly contributing levels have $l = 8$. The 16.3 MeV peak must contain a level with $l = 8$, and besides that at least one more level with lower l , most probably $l = 6$. The asymmetry of the central (90°) peak for this energy is a most peculiar effect. If the reaction we observe is described by expression (1), no other particles or photons being involved, the distribution must be symmetric around 90° . For all other energies (except maybe 12.1 MeV, see Fig. 12) the distributions never showed any significant departure from symmetry, but for 16.3 MeV the asymmetry was observed in four different measurements using three different rods and pointers.

One may try to understand the excitation curve in different ways:

1°. One may regard the peaks of the curve as being caused by individual levels in the compound nucleus. With the exception of the 15.9 MeV peak, each peak must then cover at least two levels, as discussed above.

2°. One may assume a somewhat larger number of participating levels and regard the peaks as being caused by statistical fluctuations in the level density. In some cases a peak may then correspond to one or a few strongly excited levels (for instance 15.9 MeV), but in other cases to many relatively weakly excited levels. Even in the latter cases the angular distributions may be expected to be of the type found; in expression (12) α_1 may stand for the sum of the coefficients of any number of levels with angular momentum l_1 . Considering the influence of the centrifugal barrier in the C-C system one would, if many levels are involved in each peak, expect a gradual change of the angular distributions; when the energy is increased, more levels with higher l values will contribute to the distribution. This is just what has been observed. The 12.1 MeV peak is nearly described by P_4^2 , but a small admixture of P_6 is needed to give an exact fit to the positions of the maxima. For 12.6 and 13.6 MeV gradually larger admixtures of P_6 are appropriate. For energies above 14 MeV levels with $l = 8$ begin to play a role.* This result, especially for the energy region 12–14 MeV, seems to be strongly in favour of the many-level hypothesis. Other features of the curve in Fig. 10 support this way of looking at things. If each peak corresponded to only a few levels one would expect much stronger variations in the relative peak heights. Also, if the levels were so scant that each peak covered only two or three, one would expect more cases of single levels, i. e. pure P_l^2 distributions. However, the rather deep minima in the excitation curve show that the density of participating levels cannot be very high. In this connection, it may be remarked that repeated careful investigations have shown that the cross section at 15.6 MeV is less than 2% of the cross section at 15.9 MeV. From considerations of the kind intimated above, the average spacing of participating levels may be roughly estimated to about 40 keV.

3°. A third point of view may be mentioned. One might assume a very large number of weakly excited levels giving a general, low “background”;

* The Chalk River group has measured⁸⁾ some angular distributions for the ground state α -particles from the inverse reaction in an energy range corresponding to 10–11 MeV in our scale. The distributions indicate rather low angular momenta and seem to vary rather smoothly with energy.

the peaks on top of it correspond to individual, strongly excited levels. The very small cross section at 15.6 MeV and the small variation in peak heights are in disfavour of this point of view.

These experiments were carried out at the Institute for Theoretical Physics, University of Copenhagen, and the authors wish to express their deep gratitude to the Director of the Institute, the late Professor NIELS BOHR. In conclusion we thank mag. sc. N. O. ROY POULSEN for valuable discussions, Ing. PH. DAM and Ing. A. HEDEGAARD for technical assistance.

*Institute for Theoretical Physics,
University of Copenhagen, Denmark*

References

1. D. A. BROMLEY, J. A. KUEHNER and E. ALMQUIST: Proc. Int. Conf. Nucl. Structure, Kingston, Canada. (Univ. Toronto Press and North-Holland Publishing Co. 1960), p. 255.
E. ALMQUIST, D. A. BROMLEY and J. A. KUEHNER: *ibid.* p. 258.
J. A. KUEHNER, B. WHALEN, E. ALMQUIST and D. A. BROMLEY: *ibid.* p. 261. See also Phys. Rev. Lett. **4**, 365 and 515, 1960, and Proc. Sec. Conf. Reactions between Complex Nuclei, Gatlinburgh, 1961, paper C-4, p. 151 and paper E-5, p. 282.
2. N. O. LASSEN: Nucl. Phys. **38**, 442, 1962.
3. N. O. LASSEN and Gunnar Sørensen: Nucl. Phys. **38**, 450, 1962.
4. N. O. LASSEN: Phys. Lett. **1**, 65, 1962.
5. N. O. LASSEN: Phys. Lett. **1**, 161, 1962.
6. H. W. FULBRIGHT, N. O. LASSEN and N. O. ROY POULSEN: Mat. Fys. Medd. Dan. Vid. Selsk. **31**, 10, 1959.
7. R. D. EVANS: The Atomic Nucleus, McGraw-Hill, N. Y. 1955, p. 421.
8. H. E. GOVE: Nucl. Instr. and Meth. **11**, 63, 1961.